HHS Public Access

Author manuscript

Proc SPIE Int Soc Opt Eng. Author manuscript; available in PMC 2019 July 23.

Published in final edited form as:

Proc SPIE Int Soc Opt Eng. 2018 February ; 10578: . doi:10.1117/12.2293346.

Robust Quantitative Assessment of Trabecular Microarchitecture in Extremity Cone-Beam CT Using Optimized Segmentation Algorithms

M. Brehler[a], **Q. Cao**[a], **K. F. Moseley**[b], **G. Osgood**[c], **C. Morris**[c], **S. Demehri**[d], **J. Yorkston**[e], **J. H. Siewerdsen**[a,d], **W. Zbijewski**[a]

[a]Department of Biomedical Engineering, Johns Hopkins University, Baltimore, MD USA

[b]Division of Endocrinology, Diabetes and Metabolism, Johns Hopkins University, Baltimore, MD USA

[c]Department of Orthopedics, Johns Hopkins University, Baltimore, MD USA

[d]Department of Radiology, Johns Hopkins University, Baltimore, MD USA

[e]Carestream Health, Rochester, NY USA

Abstract

Purpose: *In-vivo* evaluation of bone microarchitecture remains challenging because of limited resolution of conventional orthopaedic imaging modalities. We investigate the performance of flat-panel detector extremity Cone-Beam CT (CBCT) in quantitative analysis of trabecular bone. To enable accurate morphometry of fine trabecular bone architecture, advanced CBCT pre-processing and segmentation algorithms are developed.

Methods: The study involved 35 transilliac bone biopsy samples imaged on extremity CBCT (voxel size 75 μm, imaging dose ~13 mGy) and gold standard μCT (voxel size 7.67 μm). CBCT image segmentation was performed using (i) global Otsu's thresholding, (ii) Bernsen's local thresholding, (iii) Bernsen's local thresholding with additional histogram-based global pre-thresholding, and (iv) the same as (iii) but combined with contrast enhancement using a Laplacian Pyramid. Correlations between extremity CBCT with the different segmentation algorithms and gold standard μCT were investigated for measurements of Bone Volume over Total Volume (BV/TV), Trabecular Thickness (Tb.Th), Trabecular Spacing (Tb.Sp), and Trabecular Number (Tb.N).

Results: The combination of local thresholding with global pre-thresholding and Laplacian contrast enhancement outperformed other CBCT segmentation methods. Using this optimal segmentation scheme, strong correlation between extremity CBCT and μCT was achieved, with Pearson coefficients of 0.93 for BV/TV, 0.89 for Tb.Th, 0.91 for Tb.Sp, and 0.88 for Tb.N (all results statistically significant). Compared to a simple global CBCT segmentation using Otsu's algorithm, the advanced segmentation method achieved ~20% improvement in the correlation coefficient for Tb.Th and ~50% improvement for Tb.Sp.

Conclusions: Extremity CBCT combined with advanced image pre-processing and segmentation achieves high correlation with gold standard μCT in measurements of trabecular microstructure. This motivates ongoing development of clinical applications of extremity CBCT in *in-vivo* evaluation of bone health e.g. in early osteoarthritis and osteoporosis.

Keywords

trabecular bone; cone-beam CT; Laplacian pyramid; Trabecular segmentation; Tb.Th; Tb.Sp; Tb.N; BV/TV

1. INTRODUCTION

Trabecular microarchitecture is an important determinant of bone health. Pathological alterations of trabecular microstructure have been observed in a range of musculoskeletal disease ranging from osteoporosis[1] to osteoarthritis[2]. However, clinical utilization of microstructural measurements is currently limited to ex-vivo samples using μCT because of the insufficient spatial resolution of conventional orthopaedic imaging modalities.

Cone-Beam CT (CBCT) scanners based on flat-panel detector (FPD) technology offer a promising opportunity for development of *in-vivo* trabecular measurement capability because of the relatively high spatial resolution of FPDs (pixel sizes ~150 μm).[3] Fig. 1 illustrates a recently introduced dedicated CBCT system for imaging of the extremities.[4] The scanner uses a Varian PaxScan 2530CB FPD and achieves maximal spatial resolution of ~1.8 lp/mm (10% modulation transfer). Compared to conventional CT, the benefits of extremity CBCT include simplified logistics, ~2x lower scan dose, and the novel capability for volumetric weight-bearing imaging (Fig. 1 (a)). The system provides a convenient platform for comprehensive diagnostic evaluation of the extremities and is a compelling candidate for the development of *in-vivo* quantitative evaluation of bone microarchitecture.

Conventional approach to trabecular micromorphometry involves a segmentation step that separates the trabecular ridges from the background. This segmentation step is typically relatively straightforward in ultra-high-resolution μCT using global threshold-based segmentation algorithms, but becomes more challenging in systems with lower spatial resolution, such as extremity CBCT, due to blur and partial volume effects. We investigate advanced pre-processing and segmentation techniques to provide robust trabecular measurements in extremity CBCT. Trabecular metrics obtained with extremity CBCT are validated against gold standard micro-CT.

2. METHODS

2.1. Bone sample imaging and workflow of the evaluation study

Evaluation was performed using 35 transiliac bone biopsy samples collected in an IRB approved study of bone quality in patients with impaired glucose tolerance and type 2 diabetes mellitus. The samples were approximately 14 mm × 8 mm. Gold standard μCT images were obtained on a SkyScan 1172 system (Burker microCT, Belgium) with 7.67 μm voxel size. Extremity CBCT imaging was performed on a prototype extremity CBCT scanner using an investigational high-resolution protocol involving 420 projection views acquired with no pixel binning (137 μm pixel size) at beam energy of 90 kVp and patient dose of ~13 mGy (central CTDI dose). Total scan time was ~60 sec. Each sample was immobilized and imaged individually in a 55 mm diameter water cylinder to approximately emulate the attenuation and scatter of a human wrist (Fig. 1 (c)). In addition to the bone

sample, the cylinder contained three Bone Mineral Density (BMD) rods for calibration of measured attenuation values to local BMD. CBCT images were reconstructed on a 75 μm voxel grid using Feldkamp algorithm with Hann-apodized filter with cutoff at Nyquist frequency.

Figure 2 illustrates the procedure used to validate CBCT against gold standard μCT. For each sample, a binary mask defining a region of interest (ROI) in the trabecular bone (excluding the cortical bone) was automatically generated in the μCT image. Analysis of the metrics of bone microarchitecture was performed in this ROI. In order to find an ROI including the same region of trabecular bone in the CBCT volume, a transformation mapping the μCT volume onto the CBCT volume was first found by rigid registration with μCT as the moving image. Next, this transformation was applied to the μCT ROI mask to yield a CBCT ROI for subsequent analysis. In this manner, the metrics were measured in the original, un-transformed μCT and CBCT volumes and only the ROI mask was subject to rigid transformation and interpolation.

Four important metrics of microarchitecture[5,6] were investigated: Trabecular Spacing (Tb.Sp), Bone Volume Fraction (BV/TV), Trabecular Thickness (Tb.Th) and Trabecular Number (Tb.N). Segmentation of the trabeculae in the μCT image was performed with automatic global thresholding using the Otsu's method[7]. The CBCT volumes were segmented using the four candidate algorithms explained in the next subsection. The trabecular metrics were obtained from the segmented volumes as follows: BV/TV was the fraction of the of mineralized bone voxels (BV) over the total number of voxels in the ROI (TV). Tb.Th, which measures the thickness of the segmented trabecular ridges, and Tb.Sp, which measures the spacing between trabecular ridges, were calculated by a sphere fitting algorithm as in Ref. 5. Tb.N is the inverse of the distance between the mid-axes of the trabeculae. It was obtained using the method in Ref. 6. Tb.Th, Tb.Sp, and Tb.N are reported as mean values over the ROI.

Pearson correlation coefficient was used to compare CBCT metrics obtained using the four candidate segmentation algorithms with gold-standard μCT.

2.2 Trabecular segmentation algorithms for extremity CBCT.

The following segmentation algorithms were tested in the extremity CBCT data: global thresholding using Otsu's method[7], Bernsen's local thresholding[8] with and without an additional global pre-thresholding step based on histogram analysis, and local thresholding with Laplacian Pyramid image enhancement[9] to improve the contrast of high frequency features.

The global Otsu's method assumed a tri-modal distribution of attenuation values (air, soft-tissue, bone) and will be subsequently referred to as 2-threshold Otsu. The algorithm selects the thresholds that minimize the intra-class variance. The local thresholding with Bernsen's method used a sliding window. Window size was set to 10 based on preliminary experiments indicating balanced performance across all trabecular metrics. This windows size was also found to maximize (or nearly maximize) the dice similarity coefficients between the segmented CBCT reconstructions of the samples and their corresponding μCT

segmentations. For each window position, the center voxel was assigned to one of the two classes (bone or background) based on thresholding with the mid-grey value of the window. The thresholding step was omitted when the local contrast (max-min value) inside the window fell below a given threshold (here set to 15 after converting the image values to 8 bit integer range). In that case, the whole window was considered to be of only one class based on the mid-grey value and the class of the center voxel was assigned accordingly.

The local thresholding algorithm was next augmented by inclusion of a global pre-thresholding step (illustrated in Fig. 3). This step removes the majority of background and air voxels from the image, so that the local histogram consist mainly of bone voxels and soft-tissue voxels with elevated attenuation due to partial volume effect. To achieve the global pre-thresholding, we fit a Gaussian to the highest peak of the global histogram of the image and remove all voxel with values below the upper half width at half maximum (HWHM) of the Gaussian fit. When local segmentation is applied to such pre-thresholded image, it essentially separates partial volume soft-tissue voxels from voxels that are likely to represent “true” trabecular bone.

The final segmentation method involves the same local thresholding approach with a global pre-thresholding step, but now applied to the image enhanced with a Laplacian Pyramid. In this approach, the original image is decomposed image into a pyramid of different scale levels. A non-linear mapping function is applied to each level of the pyramid to amplify low contrast features. We used a non-linear mapping function proposed by Stahl et al.[9] The processed levels of the pyramid are then recombined into a contrast enhanced version of the original image.

By virtue of utilizing a multiscale decomposition of the image, the Laplacian Pyramid typically provides more robust contrast enhancement of features at various scales than unsharp masking (which can be considered a subset of Laplacian Pyramid techniques). This approach found broad utilization in contrast enhancement in radiography,[10,11] where the images often present a wide range of intensities. By using a Laplacian Pyramid, the contrast of features at various scales can be enhanced without saturating the gray scale range. This study investigates whether the benefits of multi-scale contract enhancement previously shown in radiographs extend to CBCT, in particular as a pre-processing step in trabecular segmentation. The Laplacian Pyramid is anticipated to aid in segmentation of e.g. the terminal segments of trabecular ridges. Due to partial volume effects, such features often present as mid-resolution, low-contrast signal that might not be adequately enhanced by conventional unsharp masking, which typically operates in a narrow high frequency channel.

We optimized the parameters of the Bernsen’s local segmentation algorithm and of the contrast enhancement transfer function in the Laplacian Pyramid by computing dice coefficients between the CBCT and micro-CT segmentations. Parameters yielding balanced performance across all samples (i.e. achieving maximal or nearly maximal value of the dice coefficient) were selected for this study. We note that a relatively broad range of parameter values yielded similar segmentation performance. Ongoing studies will investigate whether the parameters chosen in this experiment can be applied across a broad range of imaging conditions and object sizes.

3. RESULTS AND BREAKTHROUGH WORK

According to gold standard micro-CT measurements, the 35 transiliac samples covered a broad range of BV/TV values, from 7.5% to 50.5%. Figure 4 compares images and segmentations obtained with CBCT and micro-CT for three samples representing low, mid and high values of the trabecular metrics in our dataset. The micro-CT and CBCT reconstructions were registered for visual comparison (note again that the bone metrics were computed by only registering the location of the measurement ROI). Application of pre-thresholding yields generally thinner trabecular ridges compared to local thresholding without the pre-thresholding step. Laplacian enhancement provides visible improvement in the contrast of trabecular bone. The segmentation of the Laplacian enhanced image combined with local thresholding and global pre-thresholding results in further reduction of apparent trabecular thickness

Pearson correlation coefficients between CBCT and μCT for the different pre-processing and segmentation methods are shown in Table 1. The results confirm visual evaluation of Fig. 4. Simple global thresholding is outperformed by local thresholding, in particular in measurements of trabecular thickness. The addition of histogram-based global pre-thresholding provides a substantial increase in correlation with micro-CT for BV/TV, Tb.Sp and Tb.N and maintains the performance of the local methods in Tb.Th. Contrast enhancement using the Laplacian Pyramid scheme combined with pre-thresholded local segmentation yielded best correlations with μCT among the methods tested in this study, achieving values close to 0.9 for all metrics.

4. CONCLUSIONS

We investigated the performance of extremity cone-beam CT in metrics of trabecular microarchitecture. In particular, we evaluated advanced pre-processing and segmentation techniques to enable robust extraction of the trabeculae in CBCT images. A combination of local thresholding with a global pre-thresholding step and Laplacian Pyramid image enhancement was found yield the highest correlations with gold standard micro-CT for all trabecular metrics considered in this work. The application of Laplacian Pyramid was particularly beneficial for the metric of BV/TV, likely because of the enhanced contrast between bone and background across all resolution levels, which in turn decreased the number of voxels that were incorrectly segmented as trabecular ridges.

Compared to baseline global segmentation using Otsu’s method, the optimal segmentation scheme substantially improved the correlations between CBCT and μCT; the improvement in Pearson correlation coefficient was ~22% for BV/TV, ~27% for Tb.Th, ~56% for Tb.Sp, and ~31% for Tb.N. Overall, correlations of ~0.9 were achieved for all investigated trabecular metrics after the application of image enhancement and local thresholding. Such high correlations with pre-clinical μCT indicate that extremity CBCT may find utility in detection of changes in bone microstructure induced by disease or therapeutic intervention.

Ongoing work involves pilot patient studies in detection of radiation-induced bone loss during radiotherapy and in early osteoarthritis, as well as additional evaluation in bone

samples and correlation of CBCT-based microstructural metrics with measurements of mechanical properties of bone. Parallel technical development includes motion compensation algorithms[12] and investigation of new higher resolution FPDs based on CMOS technology.[13]

ACKNOWLEDGEMENTS

This work was supported by NIH Grants R01-EB-018896, R21-CA-208821, and collaboration with the Carestream Health (Rochester NY).

REFERENCES

[1]. Parfítt AM, Mathews CH, Villanueva AR, Kleerekoper M, Frame B, & Rao DS, “Relationships between surface, volume, and thickness of iliac trabecular bone in aging and in osteoporosis. Implications for the microanatomic and cellular mechanisms of bone loss.” Journal of clinical investigation, 72(4), 1396 (1983). [PubMed: 6630513]

[2]. Weinans H, Siebelt M, Agricola R, Botter SM, Piscaer TM, Waarsing JH, “Pathophysiology of peri-articular bone changes in osteoarthritis” Bone, 51, 190–196 (2012). [PubMed: 22343134]

[3]. Klintström E, Smedby Ö, Moreno R and Brismar TB, “Trabecular bone structure parameters from 3D image processing of clinical multi-slice and cone-beam computed tomography data” Skeletal Radiol, 43:197–204 (2014). [PubMed: 24271010]

[4]. Carrino JA, A1 Muhit A, Zbijewski W, Thawait GK, Stayman JW, Packard N, Senn R, Yang D, Foos DH, Yorkston J and Siewerdsen JH, “Dedicated cone-beam CT system for extremity imaging,” Radiology, 270(3), 816–824 (2013). [PubMed: 24475803]

[5]. Hildebrand T and Rüegsegger P, “A new method for the model-independent assessment of thickness in three-dimensional images.” J Microscopy, 185(l):67–75 (1997).

[6]. Laib A and Rüegsegger P, “Comparision of structure extraction methods for in vivo trabecular bone measurements” Computerized Medical Imaging and Graphics, 23: 69–74 (1999). [PubMed: 10227372]

[7]. Otsu N, “A threshold selection method from gray-level histograms,” Automatica, 11(285–296), 23–27 (1975).

[8]. Bernsen J, “Dynamic Thresholding of Grey-Level Images”, Proc. of the 8th Int. Conf. on Pattern Recognition (1986).

[9]. Stahl M, Aach T, Buzug TM, Dippel S and Neitzel U, “Noise-resistant weak-structure enhancement for digital radiography,” in Proc. SPIE Med. Imag, 3661: 1406–1417 (1999).

[10]. Vuylsteke P, and Schoeters EP, “Multiscale image contrast amplification (MUSICA)” in Medical Imaging 1994: Image Processing, vol. 2167, pp. 551–561. International Society for Optics and Photonics (1994).

[11]. Stahl M, Aach T, and Dippel S, “Digital radiography enhancement by nonlinear multiscale processing” Medical physics 27, no. 1: 56–65 (2000).

[12]. Sisniega A, Stayman JW, Yorkston J, Siewerdsen JH, Zbijewski W, “Motion compensation in extremity cone-beam CT using a penalized image sharpness criterion”, Physics in medicine and biology 62 (9), 3712 (2017). [PubMed: 28327471]

[13]. Cao Q, Brehler M, Sisniega A, Stayman JW, Yorkston J, Siewerdsen JH and Zbijewski W, “High-resolution extremity cone-beam CT with a CMOS detector: task-based optimization of scintillator thickness”, in Medical Imaging 2017: Physics of Medical Imaging, Proceedings of SPIE Vol. 10132, 1013210 (2017).

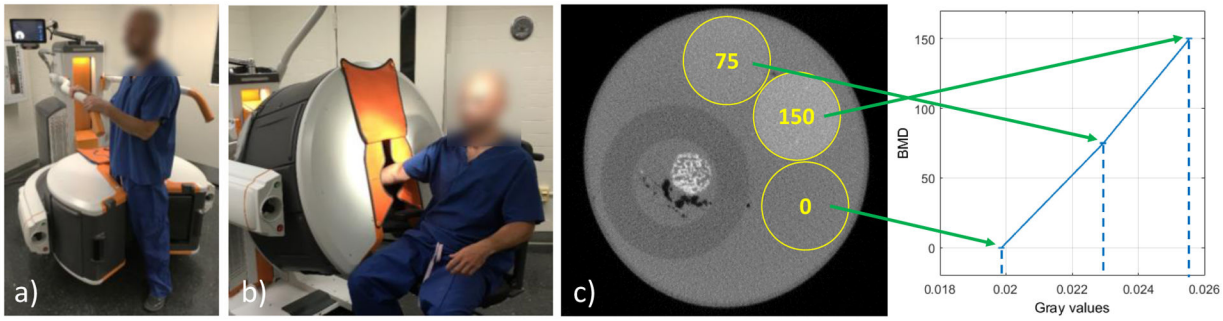

Figure 1.

Dedicated extremity CBCT (Carestream OnSight 3D), a) Standing configuration for weight-bearing imaging of lower extremity (foot, ankle, knee), b) Sitting configuration for imaging of hand, wrist and elbow and now-weight-bearing lower extremities. c) Experimental setup showing axial slice with bone sample in water filled container and three bone mineral density (BMD) rods (yellow circles). The plot shows the reconstructed attenuation values of the rods versus their nominal BMD, confirming the linearity of the system.

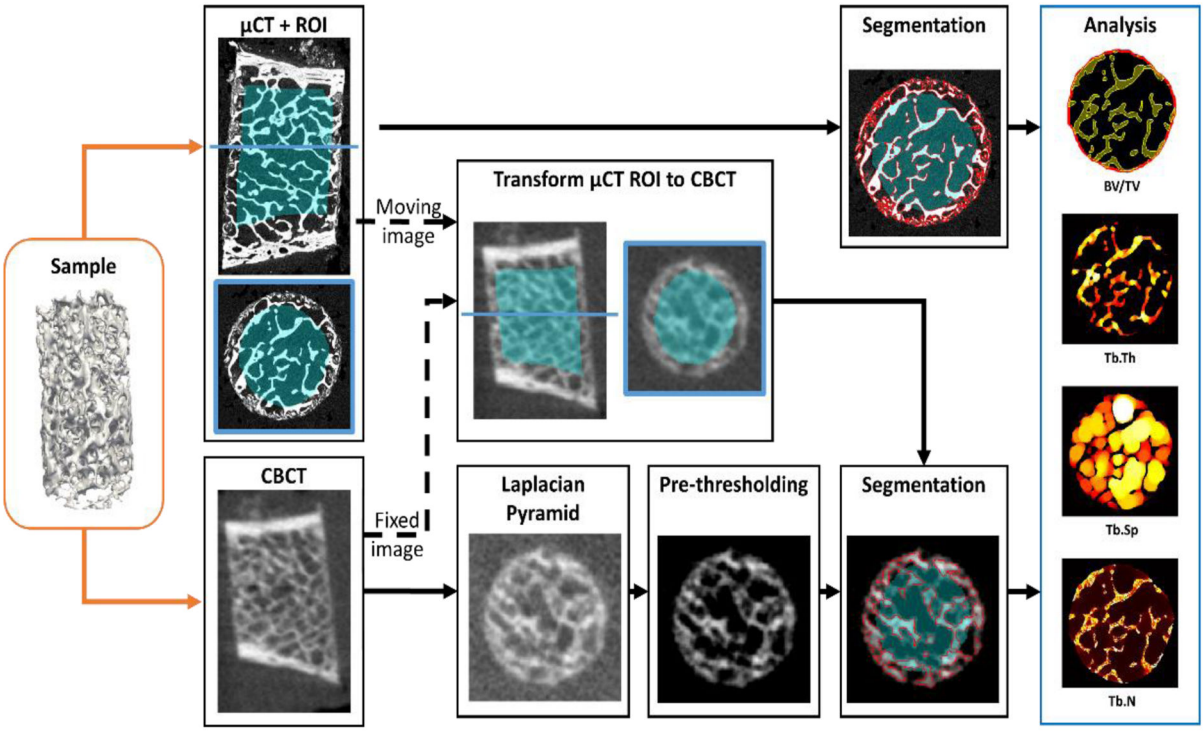

Figure 2.

Workflow of the evaluation study. Each bone sample was imaged on extremity CBCT and gold standard µCT. A binary trabecular mask was created in the µCT volume and transformed to the CBCT volume to generate ROIs for analysis of metrics of trabecular microstructure. To enable robust trabecular measurements in CBCT, segmentation algorithms ranging from global Otsu's thresholding to local thresholding with Laplacian Pyramid image enhancement were evaluated.

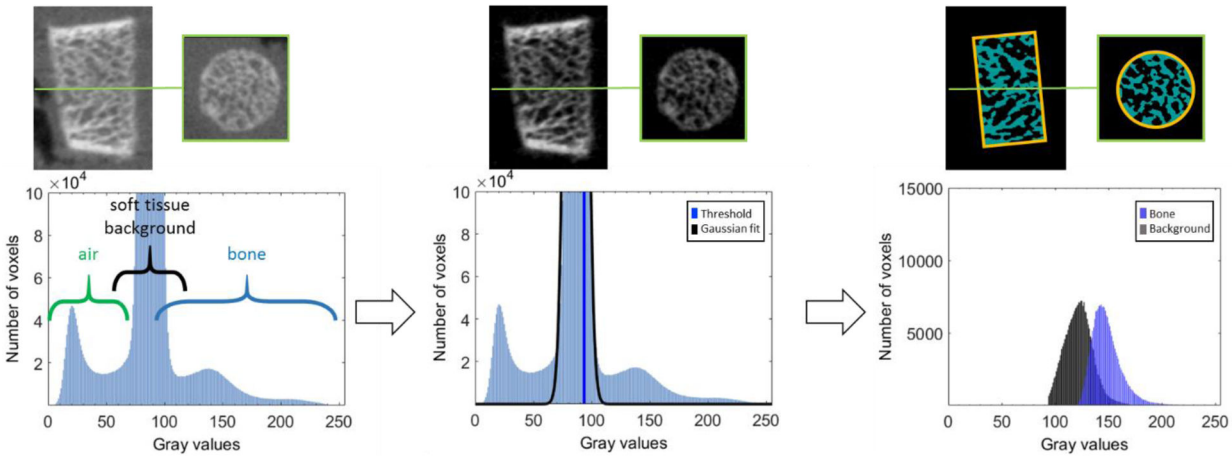

Figure 3.

Histogram-based pre-thresholding. Each sample can be roughly separated into three classes: air, soft tissue background and bone voxels (left). By fitting a Gaussian to the highest peak of the histogram and calculating the upper half width at half maximum of the Gaussian fit, the bone voxels are separated from air and most of the soft tissue background (center). Inside the ROI used for calculation of the morphological metrics of trabecular microstructure, the local segmentation provides further separation of the pre-thresholded voxels into two classes (right).

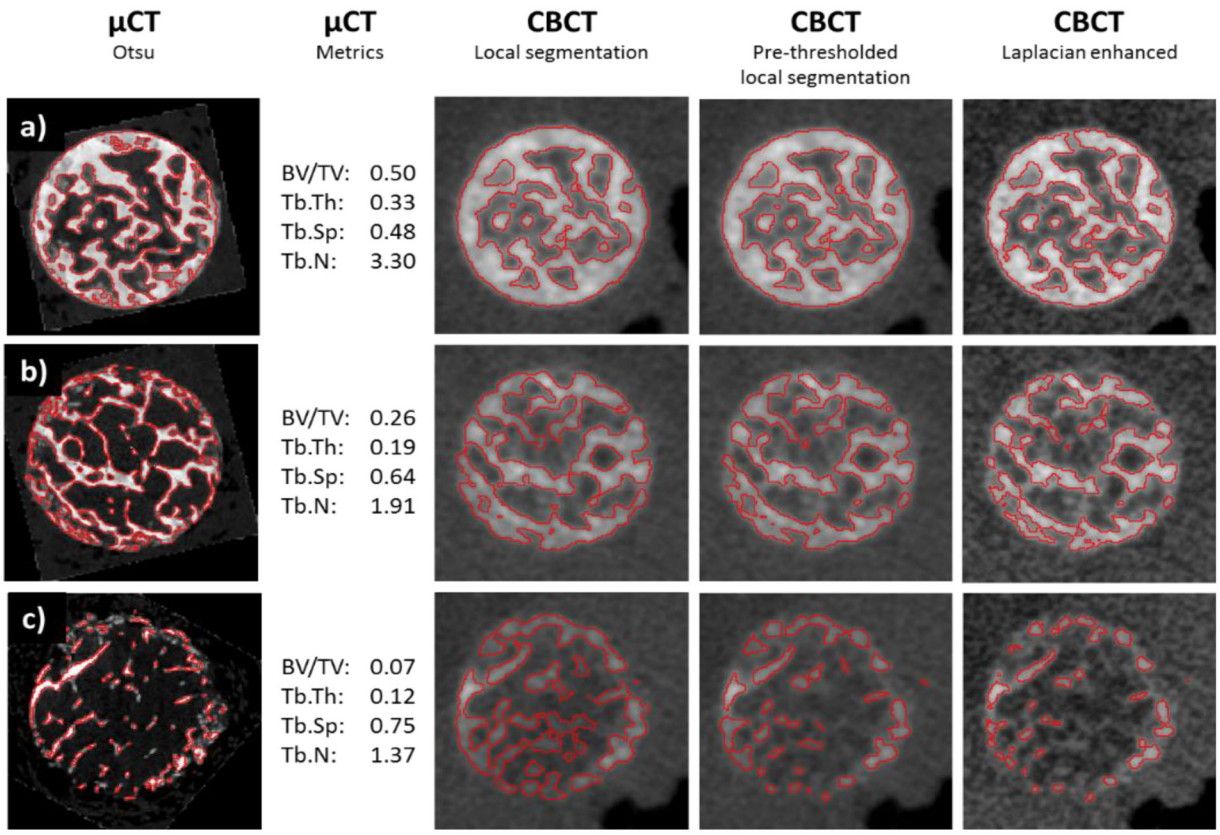

Figure 4.

Comparison of three samples (a, b and c) imaged on µCT and CBCT and processed with different pre-processing and segmentation methods. First column shows axial view of µCT images with an overlay of a global Otsu's segmentation. Values of trabecular metrics are also provided. The subsequent columns show the same sample imaged on extremity CBCT and segmented using local thresholding, local thresholding with a global pre-thresholding step, and Laplacian-enhanced local thresholding. To facilitate visual comparison, µCT images were registered to CBCT.

Table 1

Pearson correlation coefficients between CBCT-based measurements and gold-standard micro-CT for 35 transiliac bone biopsy samples. The rows represents the four CBCT segmentation algorithms proposed in this study.

Algorithm	BV/TV	Tb.Th	Tb.Sp	Tb.N
2-Threshold Otsu	0.76	0.70	0.58	0.67
Local	0.78	0.85	0.64	0.67
Pre-thresholded Local	0.89	0.85	0.90	0.87
Pre-thresholded Local Laplacian	0.93	0.89	0.91	0.88